

THE INFLUENCE OF THE SUBSTRATE TEMPERATURE ON THE STRUCTURE AND ON THE OPTICAL ENERGY BANDGAP OF BISMUTH OXIDE THIN FILMS PREPARED BY PULSED LASER DEPOSITION

S. CONDURACHE-BOTA^{a*}, C. CONSTANTINESCU^b, M. PRAISLER^a,
N. TIGAU^a

^a*Dunarea de Jos University of Galati, Faculty of Sciences and Environment,
111 Domneasca Street, 800201, Galati, Romania*

^b*National Institute for Laser, Plasma and Radiation Physics - INFLPR, PPAM –
Lasers Department, 409 Atomistilor Blvd., Magurele 077125, Bucharest, Romania*

Radiofrequency-assisted pulsed laser ablation (RF-PLD) can be used for the preparation of a large range of thin films, including oxides. This paper presents the results of the analysis of bismuth oxide thin films deposited by RF-PLD on glass substrates maintained at different temperatures, between 300 deg. C and 600 deg. C. X-ray diffraction studies revealed both the composition and the structure of the films, which proved to be polycrystalline, with some bismuth trioxide polymorphs and with coexisting non-stoichiometric bismuth oxides. The optical energy bandgaps, E_g of the films are inferred and their values are discussed as related to the composition and structure of the films, as changing with the substrate temperature.

(Received June 15, 2015; Accepted September 3, 2015)

Keywords: Pulsed laser deposition, Polymorphism, Non-stoichiometric Bismuth oxides, Energy bandgap, Substrate temperature

1. Introduction

Thin semiconducting films are a part of our life, from the displays of TV sets to phones, from CD's and DVD's to solar cells. And since the need of such materials is continuously growing as the technology advanced, scientists keep searching for them, as well as for the most versatile preparation methods, capable of giving those semiconducting films most adequate for specific applications [1-6].

Bismuth oxide thin films are among such semiconducting materials with photosensitivity, large energy bandgap and high refractive index as trioxide, making them useful for various applications as optical coatings, solar or fuel cells, microwave integrated circuits and/or gas sensors [1, 7-9].

The oxidation of pure bismuth as depositing on a substrate proves to be cheaper than using bismuth oxide as starting substance, due to the price of the materials themselves. Still, upon oxidation, bismuth can form various intermediate oxides, such as $\text{BiO}_{1.5}$ and $\text{Bi}_2\text{O}_{2.33}$, as well as several polymorphs of bismuth trioxide, Bi_2O_3 , from which the most encountered are: α - Bi_2O_3 (stable, monoclinic), β - Bi_2O_3 (metastable, tetragonal) and δ - Bi_2O_3 (stable, face-centered cubic). The overall composition and structure of such oxides mixtures strongly depend on the preparation method and conditions, among which the nature of the substrate and its temperature upon deposition of the oxide are essential [10-13].

Here we analyse how the temperature of the glass substrate during the deposition of thin bismuth oxide films influence their structure and their energy bandgaps when one uses as preparation technique: pulsed laser ablation (PLD) of pure bismuth targets in radiofrequency-

*Corresponding author: scondurache@ugal.ro

induced oxygen plasma within the ablation chamber. This technique makes use of the possibility to concentrate high-energy laser radiation on small areas of a target, such that material from it would evaporate (if it is initially liquid) or would even sublime (in case of a solid target) and subsequently would deposit on a substrate placed closely to the target (at centimetres range). Pulsed laser ablation was already successfully applied for the preparation of various types of thin films [14-16].

2. Experimental

An Ar:F excimer LASER device from *Coherent GmbH* was used for ablation, producing pulses with $\lambda = 193$ nm, 10 Hz repetition frequency and 270 mJ/pulse. A *Caesar* 1310 RF source, with 13.56 MHz frequency and 100 W power was used to induce oxygen plasma within the ablation chamber.

The targets were made of pure bismuth (99.999%) from *Merck* and high-quality BK-7 microscope glass slides were the substrates of choice, which were thoroughly cleaned with high-purity alcohol prior to the depositions.

The oxygen flux inside the ablation chamber was set to 100 sccm, at 0.6 mbar partial pressure.

As stated above, the substrates were kept at different temperatures during thin film depositions, namely: room temperature (RT, i.e. 27 deg. Celsius), 300, 400, 500 and 600 deg. Celsius, respectively.

The structural information was inferred from the X-ray diffraction (XRD) data, by using a DRON 3 diffractometer, operating with the Cobalt K_{α} line ($\lambda_x = 1.789$ Å), in a two theta arrangement. According to Bragg's relation, the interplanar distances between the types of parallel crystalline planes within the films were computed as:

$$d = \frac{\lambda_x}{2 \cdot \sin \theta} \quad (1)$$

where θ denoted the diffraction angle corresponding to a certain XRD peak (a X-ray diffraction maximum).

A Perkin Elmer Lambda 35 spectrophotometer was used for optical transmittance and reflectance measurements within 190 – 1100 nm spectral range, from which the absorption coefficient, α was computed. Then, Tauc's model was applied in order to determine the energy bandgap, E_g of the deposited films, according to [17,18]:

$$(\alpha \cdot h \cdot \nu)^r = A \cdot (h \cdot \nu - E_g) \quad (2)$$

with $h\nu$ denoting photon energy, A - an energy-independent constant and r - an index related to the type of optical absorption process within the film, as given in the table below:

Table 1. Correspondence between the value of index r and the type of optical absorption process within Tauc's model

Crt. No.	Value of coefficient r	Type of optical transition
1.	2	allowed direct transition
2.	1/2	allowed indirect transition
3.	2/3	forbidden direct transition
4.	1/3	forbidden indirect transition

3. Results and discussion

Following the recording of the X-ray diffraction spectra, the interplanar distances between the parallel crystalline planes of the deposited films were computed, according to (1). Subsequently, by using the JCPDS diffraction database [19-30], the diffraction peaks were identified both from the point of view of the substance to which they belong to and as the Miller indices are concerned (see Fig.1).

When interpreting the data, one has to consider the influence of target erosion subsequent to repeated ablations, giving raise to slightly different sublimation efficiency of the target material and thus, influencing both the thickness and the oxidation degree and depth of the films while depositing on the glass substrate.

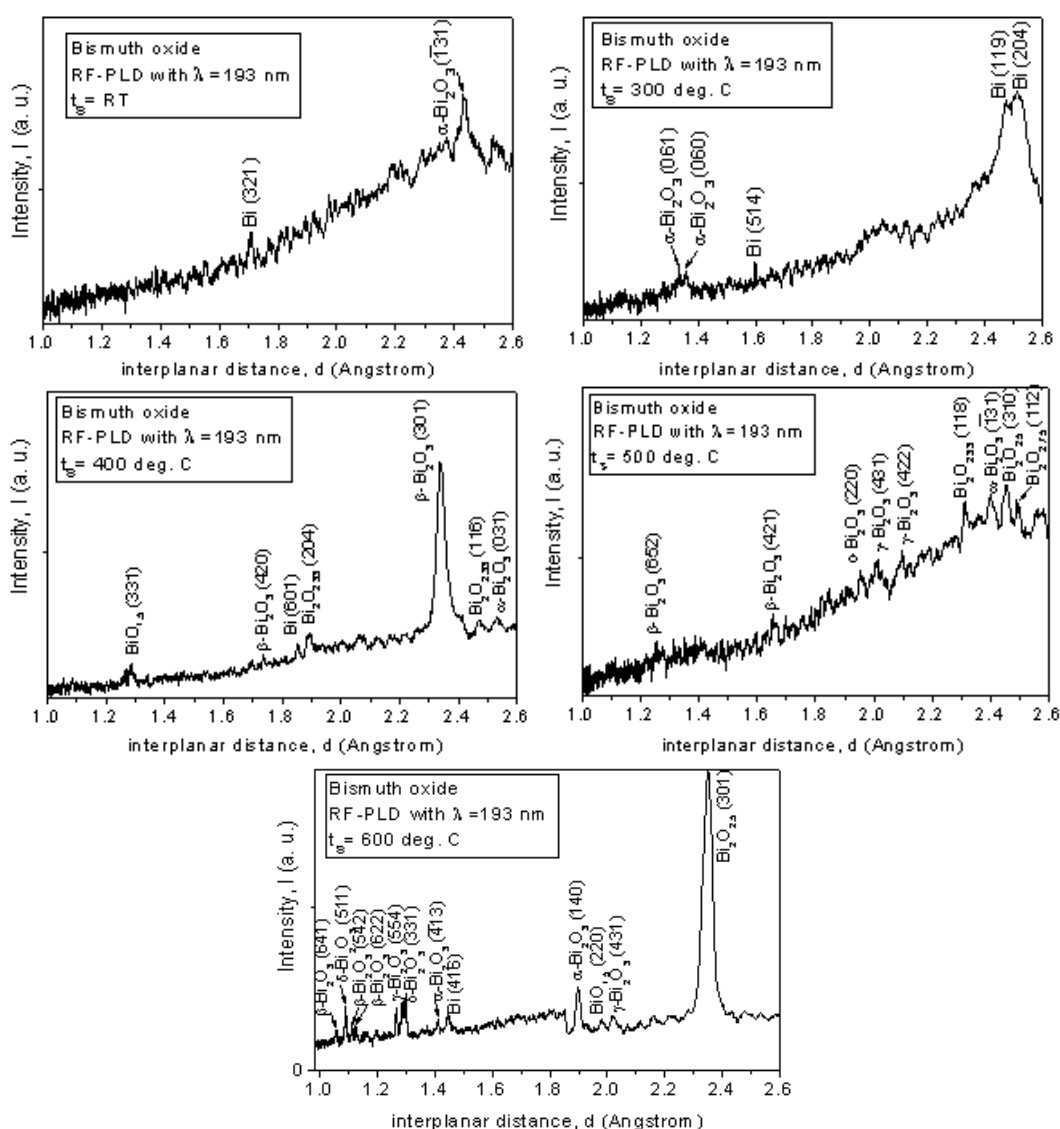


Fig. 1 X-ray diffraction spectra for each of the bismuth oxide thin films prepared by RF-PLD with $\lambda=193$ nm laser pulses

Thus, the XRD spectra from Fig. 1 prove that bismuth oxidation happened in the deposited films, no matter what the temperature of the substrate was (either small – RT – or high – up till 600 deg. C), since the alpha phase of bismuth trioxide appears in each XRD spectrum. Still, the crystalline planes of α - Bi_2O_3 formed in the films are changing as the substrate temperature, t_s was

changes. Thus, while $(\bar{1}31)$ formed at $t_s = \text{RT}$ and at 500 deg. C, instead (061) planes appeared for $t_s = 300$ deg. C, while (031) planes formed at $t_s = 400$ deg. C and $(\bar{4}13)$ planes appeared at $t_s = 600$ deg. C.

Also, one can notice the complete bismuth oxidation for $t_s = 500$ deg. C, since no pure Bi XRD peak was identified in the corresponding spectrum, in contrast with the other analysed films, exhibiting small diffraction peaks (i.e. (321) for $t_s = \text{RT}$, (514) for $t_s = 300$ deg. C, (601) for $t_s = 400$ deg. C and (416) for $t_s = 600$ deg. C). The metastable, tetragonal $\beta\text{-Bi}_2\text{O}_3$ was formed only at higher substrate temperatures, namely at 400, 500 and 600 deg. C, respectively, while crystalline planes (i.e. (511) and (331)) of the stable, face-centered cubic $\delta\text{-Bi}_2\text{O}_3$ polymorph were identified only for $t_s = 600$ deg. C.

Non-stoichiometric bismuth oxides did not form at lower substrate temperatures, i.e. at R and 300 deg. C, while the metastable, volume-centered cubic $\gamma\text{-Bi}_2\text{O}_3$ was identified only at the highest substrate temperatures set within the ablations, namely for $t_s = 500$ and 600 deg. C, respectively.

The films deposited at $t_s = 400$ and 600 deg. C present good texturing degree, as compared to the other films. It can be also noticed that the oxidation degree increases with substrate temperature for the applied RF-PLD technique, in a similar manner to what was obtained when preparing bismuth oxide films by thermal oxidation in air of pure bismuth films [10,12,13].

The optical analysis of the deposited bismuth oxide thin films focused on two key features. One was to determine the energy bandgap, which is a key parameter for a semiconductor, since it gives its specific optical absorption spectral range, but it also represents the necessary energy to induce electrical conduction in the intrinsic material. The other feature was to infer the type of optical transitions happening in the films, both because these represent an indication of the reciprocal positions of the extremes of the valence and conduction bands in the Brillouin zone and also because it strongly influence light absorption efficiency in what the photovoltaic applications of the semiconductor material under study.

Thus, according to Tauc's formula, given above as (2), all four types of optical transitions were studied for the RF-PLD deposited films, namely for: allowed direct and indirect optical transitions and for the forbidden direct and indirect optical transitions, as showed in Figs. 2-6, for the most relevant parts of the absorption spectra ion what the energy bandgap determination is concerned.

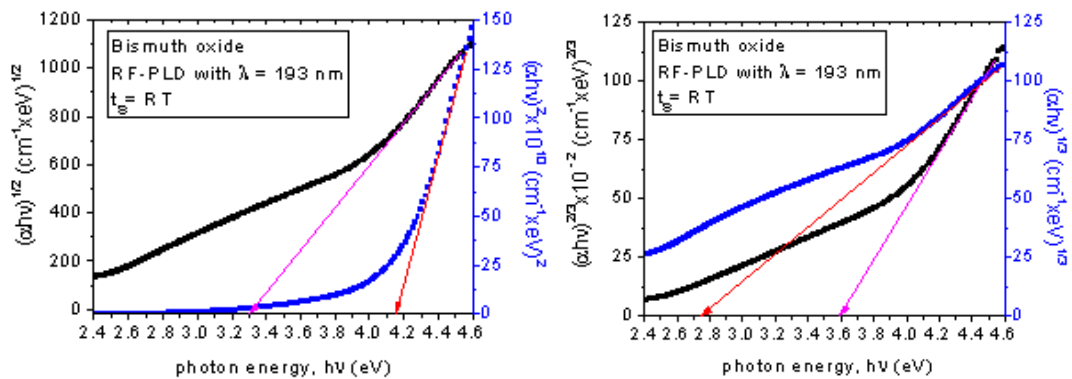


Fig. 2 Optical absorption spectra, according to Tauc's model for the bismuth oxide film deposited by RF-PLD with $\lambda=193$ nm laser pulses at $t_s = \text{RT}$

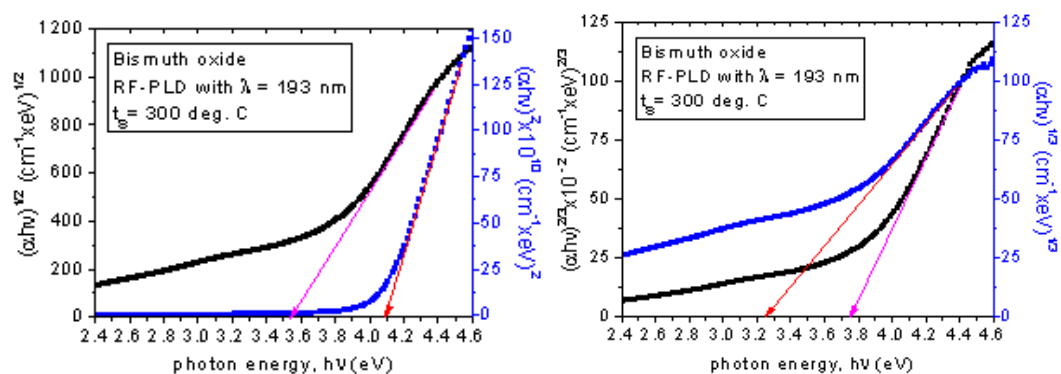


Fig. 3 Optical absorption spectra, according to Tauc's model for the bismuth oxide film deposited by RF-PLD with $\lambda=193$ nm laser pulses at $t_s = 300$ deg. C

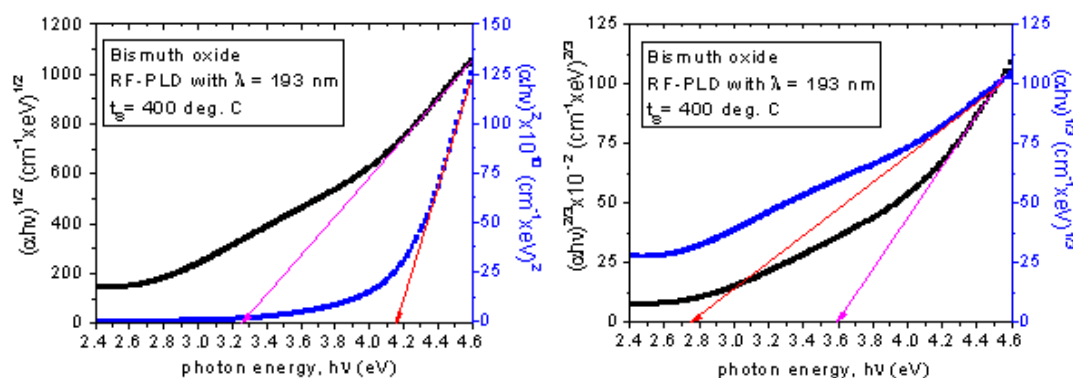


Fig. 4 Optical absorption spectra, according to Tauc's model for the bismuth oxide film deposited by RF-PLD with $\lambda=193$ nm laser pulses at $t_s = 400$ deg. C

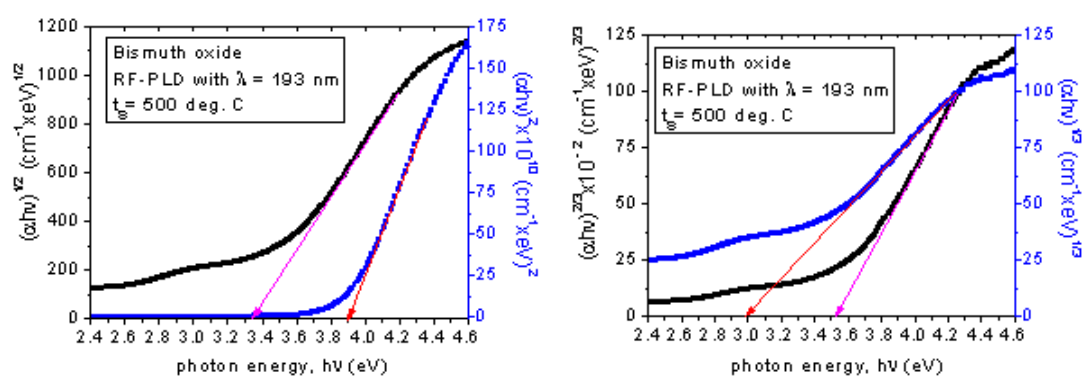


Fig. 5 Optical absorption spectra, according to Tauc's model for the bismuth oxide film deposited by RF-PLD with $\lambda=193$ nm laser pulses at $t_s = 500$ deg. C

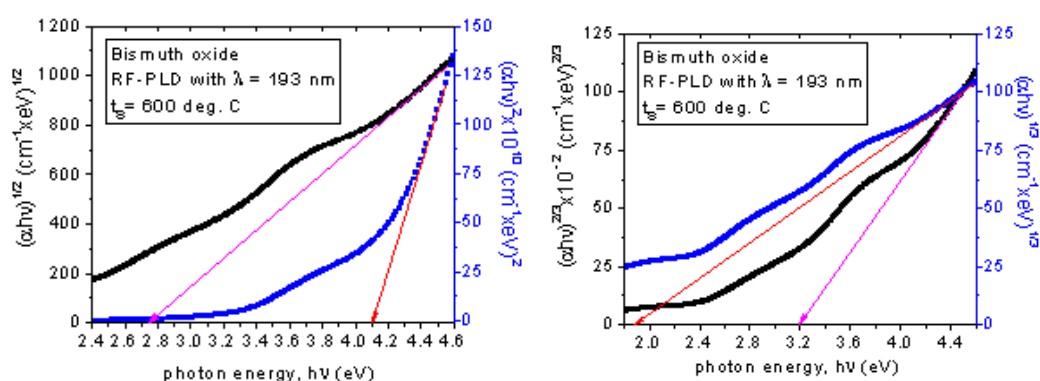


Fig. 6 Optical absorption spectra, according to Tauc's model for the bismuth oxide film deposited by RF-PLD with $\lambda=193$ nm laser pulses at $t_s = 600$ deg. C

The results of the application of Tauc's model, as obtained from Figs. 2-6 are given in Table 2 for all types of optical transitions, as explained above. It can be readily noticed that both allowed and forbidden transitions are happening within the analysed films, both as indirect and direct. The energy bandgap of each type of optical transition changes with the composition and the structure of the films, decreasing with increasing oxidation degree, especially for indirect allowed and direct forbidden transitions. This behaviour can be explained by the complex composition and structure of the films, containing a mixture of bismuth trioxide, intermediate (non-stoichiometric) oxides and remaining unoxidized bismuth in a polymorph and polycrystalline structure, giving rise to complex valence and conduction bands, with several local extremes (peaks and valleys), such as both phonon-assisted and phonon-free optical transitions happen in the films.

Table 2. The values of the energy bandgap for each possible optical transitions of the bismuth oxide films under study

Crt. No.	t_s (deg. C)	E_g (eV)			
		indirect allowed $(\alpha \cdot h \cdot \nu)^{1/2}$	direct allowed $(\alpha \cdot h \cdot \nu)^2$	indirect forbidden $(\alpha \cdot h \cdot \nu)^{2/3}$	direct forbidden $(\alpha \cdot h \cdot \nu)^{1/3}$
1.	RT	3.30	4.15	3.60	2.75
2.	300	3.55	4.10	3.75	3.25
3.	400	3.25	4.15	3.60	2.75
4.	500	3.35	3.90	3.52	3.00
5.	600	2.75	4.10	3.19	1.88

Such results were also reported by other scientists upon bismuth oxidation, prior to thermal treatment [10,11,13]. But even though annealing is performed, it can insure only the complete oxidation of bismuth, but it is not a guarantee that polymorphism is removed, since the phase transitions of bismuth trioxide can occur easily from one polymorph to another and the result of the annealing process is directly related to the initial grain structure of the films, as they are exerting reciprocal influences when heating and cooling, such that internal arrangement changes are limited by the constraints of the surrounding grains.

From the values of E_g presented in Table 2 it can be noticed that the gaps between the limits of the conduction and valence bands of the prepared films lie between 3-4 eV (i.e. up till UV), as found by others [7, 10-13], feature that recommends these films for solar energy conversion. It can be seen that the smallest values for E_g are obtained for direct forbidden transitions, while the highest E_g is inferred for direct allowed optical transitions. The films deposited at RT and at $t_s = 400$ deg. C show similar values of E_g , even though their structures are

not similar. The film deposited at the highest substrate temperature (600 deg. C) during the RF-PLD, having the most complex structure, as obtained from the XRD analysis, exhibits the smallest values for the energy bandgap for 3 out of all 4 types of optical transitions, i.e. with the exception of direct allowed transitions.

4. Conclusions

Radiofrequency-assisted pulsed laser deposition can be successfully used for the deposition of crystalline, semiconducting bismuth oxide films. The prepared films are polycrystalline and polymorph and bismuth is incompletely oxidized at any substrate temperature, which represent one of its characteristics when oxidized, no matter the applied technique [10,12,13].

All 4 types of optical transitions happen in all the analysed films, the energy bandgap being generally comprised between 3 and 4 electron-Volts. As expected, E_g changes with the composition and the structure of the films.

A higher substrate temperature improves the oxidation degree and the crystallinity, while blue shifting the energy bandgap downwards, where the solar energy is at its maximum, recommending these films for energy conversion.

Acknowledgements

The work has been funded by the Sectoral Operational Programme Human Resources Development 2007-2013 of the Ministry of European Funds through the Financial Agreement POSDRU/159/1.5/S/132397. The authors thank professor Constantin Gheorghies for the XRD measurements.

References

- [1] F. Qin, G. Li, R. Wang, J. Wu, H. Sun, R. Chen, *Chem. Eur. J.* **18**, 16491 (2012).
- [2] C. Ravariu, L.G. Alecu, A. Bondarciuc, F. Babarada, *J. Optoelectron. Adv. M.-Rapid Com.* **4**(9), 1375 (2010).
- [3] A.P. Rambu, N. Iftimie, V. Nica, M. Dobromir, S. Tascu, *Superlattice. Microst.* **78**, 61 (2015).
- [4] S.U. Offiah, P.E. Ugwoke, A.B.C. Ekwealor, S.C. Ezugwu, R.U. Osuji, F.I. Ezema, *Dig. J. Nanomater. Bios.* **7**(1), 165 (2012).
- [5] F. Tudorache, P.D. Popa, M. Dobromir, F. Iacomi, *J. Mater. Sci. Eng. B* **178**, 1334 (2013).
- [6] M.H. Ehsan, H. Rezagholipour Dizaji, M.H. Mirhaj, *Dig. J. Nanomater. Bios.* **7**(2), 629 (2012).
- [7] J. Morasch, S. Li, J. Brotz, W. Jaegermann, A. Klein, *Phys. Status Solidi A* **211** (10), 93 (2014).
- [8] F. Tudorache, I. Petrila, S. Condurache-Bota, C. Constantinescu, M. Praisler, *Superlattice. Microst.* **77**, 276 (2015).
- [9] S.S. Bhande, R. S. Mane, A.V. Ghule, S.-H. Han, *Scripta Mater.* **65**, 1081 (2011).
- [10] R. B. Patil, R. K. Puri, V. Puri, *Appl. Surf. Sci.* **253**, 8682 (2007).
- [11] R. A. Ismail, *e-J. Surf. Sci. Nanotech.* **4**, 563 (2006).
- [12] S. Condurache-Bota, N. Tigau, A. P. Râmbu, G. G. Rusu, G. I. Rusu, *Appl. Surf. Sci.* **257**, 10545 (2011).
- [13] L. Leontie, M. Caraman, M. Delibas, G. I. Rusu, *Mater. Res. Bull.* **36** (9), 1629 (2001).
- [14] M. Ion, C. Berbecaru, S. Iftimie, M. Filipescu, M. Dinescu, S. Antohe, *Dig. J. Nanomater. Bios.* **7**(4), 1609 (2012).
- [15] Leontie L., Caraman M., Visinoiu A., Rusu G. I., *Thin Solid Films* **473**, 230 (2005).
- [16] H.-U. Krebs, M. Weisheit, J. Faupel, E. Suske, T. Scharf, C. Fuhse, M. Stormer, K. Sturm,

M. Seibt, H. Kijewski, D. Nelke, E. Panchenko, M. Buback, *Adv. Solid State Phys.* **43**, 505 (2003).

[17] Z. Jiang, Y. Geng, D. Gu, *Chin. Opt. Lett.* **6**, 294 (2008).

[18] F. Yakuphanoglu, H. Erten, *Opt. Appl.* **34** (4), 969 (2005).

[19] JCPDS data files nos. 01-0688, 05-0519, 85-1329 and 44-1246 for Bi.

[20] JCPDS data files nos. 41-1449, 71-0465, 71-2274, 72-0398 and 76-1730 for α -Bi₂O₃.

[21] JCPDS data files nos. 18-244, 27-50, 29-236, 74-1374, 74-2351 and 78-1793 for β -Bi₂O₃.

[22] JCPDS data files nos. 45-1344, 71-0467 and 74-1375 for γ -Bi₂O₃.

[23] JCPDS data files nos. 16-654, 27-52, 71-0466, 74-1633, 77-0374 and 74-1633 for δ -Bi₂O₃.

[24] JCPDS data files nos. 27-54 and 75-0995 for BiO.

[25] JCPDS data file no. 78-0736 for BiO_{1.5}.

[26] JCPDS data file no. 83-0410 for Bi₂O₄.

[27] JCPDS data file no. 27-51 Bi₂O_{2.33}.

[28] JCPDS data file no. 74-1999 Bi₂O_{2.5}.

[29] JCPDS data file no. 27-49 Bi₂O_{2.75}.

[30] JCPDS data files nos. 47-1058 and 74-2352 for Bi₄O₇.